



## Article

# Risk Assessment of Toxic Gas Dispersion from Electric Vehicle Fires in Underground Apartment Parking Garages Using Numerical Analysis

Jiseong Jang <sup>1,2</sup>, Joonho Jeon <sup>3,\*</sup>  and Chang Bo Oh <sup>1,\*</sup> 

<sup>1</sup> Department of Safety Engineering, Pukyong National University, Busan 48513, Republic of Korea; jiseong@kosha.or.kr

<sup>2</sup> Department of Protective Device Certification, Korea Occupational Safety and Health Agency, Ulsan 44429, Republic of Korea

<sup>3</sup> Department of Fire Protection Engineering, Pukyong National University, Busan 48513, Republic of Korea

\* Correspondence: jeonj@pknu.ac.kr (J.J.); cboh@pknu.ac.kr (C.B.O.)

**Abstract:** With the rising adoption of electric vehicles (EVs), fire-related issues have garnered significant attention, prompting extensive research efforts. This study investigates the dispersion of toxic gases generated during EV fires in confined spaces, such as underground parking garages, to enhance fire safety protocols. Using the fire dynamics simulator (FDS), simulations were conducted for 24 kWh, 53 kWh, and 99.8 kWh battery scenarios to assess the impact of increasing battery capacities on toxic gas emissions. The results indicate that hydrogen fluoride (HF) concentrations in poorly ventilated areas peaked at 488.2 ppm, significantly exceeding the Acute Exposure Guideline Level (AEGL-2) threshold of 12 ppm. The exposure time exceeding AEGL-2 (30 min) was recorded as 53 min and 49 s for the 99.8 kWh scenario, highlighting a substantial risk to occupants and emergency responders. Additionally, the fractional effective dose (FED) for asphyxiant gases and the fractional effective concentration (FEC) for irritant gases were analyzed, revealing that larger battery capacities and proximity to the fire source reduced tenability time by up to 47% compared to smaller batteries. These findings provide critical insights into fire safety measures, emphasizing the necessity of early fire detection systems, enhanced ventilation strategies, and battery-specific fire suppression technologies in confined environments.

**Keywords:** EV fires; fire dynamics simulator (FDS); fractional effective dose (FED); fractional effective concentration (FEC); hydrogen fluoride (HF); toxic gas dispersion



Academic Editors: Wei Wang and Ying Zhang

Received: 15 January 2025

Revised: 17 February 2025

Accepted: 22 February 2025

Published: 25 February 2025

**Citation:** Jang, J.; Jeon, J.; Oh, C.B. Risk Assessment of Toxic Gas Dispersion from Electric Vehicle Fires in Underground Apartment Parking Garages Using Numerical Analysis. *Fire* **2025**, *8*, 96. <https://doi.org/10.3390/fire8030096>

**Copyright:** © 2025 by the authors. Licensee MDPI, Basel, Switzerland. This article is an open access article distributed under the terms and conditions of the Creative Commons Attribution (CC BY) license (<https://creativecommons.org/licenses/by/4.0/>).

## 1. Introduction

In recent years, global warming has led to abnormal climate events worldwide, raising significant concerns about safety risks, including those posed by electric vehicle fires. As one solution, efforts to suppress the use of fossil fuels and develop alternative energy sources have been expanding. In this context, carbon neutrality policies have been promoted, and many countries, including the EU, are transitioning to green economies. This shift has brought attention to renewable energy and environmentally friendly mobility solutions, such as electric and hydrogen vehicles, while also highlighting the need to address risks associated with their integration into confined spaces like underground parking garages. To adapt to these rapidly changing policies, both emerging electric vehicle manufacturers and traditional internal combustion engine companies are competing to develop and launch electric vehicles.

Over the past decade, the electric vehicle market has grown rapidly, and this growth is expected to continue. As of 2023, the number of registered electric vehicles in South Korea reached 543,900, accounting for 2.09% of all registered vehicles. This market is projected to expand further in the coming years [1]. However, as the market share of electric vehicles increases, so too does the scale of human and material damage caused by electric vehicle fires. In South Korea, the number of electric vehicle fires has risen significantly since 2020, coinciding with rapid adoption rates (11 cases in 2020, 24 in 2021, 44 in 2022, and 72 in 2023) [2].

Electric vehicle fires are characterized by the significant dispersion of toxic gases, distinguishing them from internal combustion engine vehicle fires. A particular concern is the release of toxic gases from lithium-ion batteries during fires [3]. Previous studies have identified hydrogen fluoride (HF) as a highly toxic and corrosive gas released when lithium salts ( $\text{LiPF}_6$ ), used as electrolytes, react with water [4,5]. HF has an ERPG-2 (Emergency Response Planning Guideline Level 2) threshold of 20 ppm and an AEGL-2 (Acute Exposure Guideline Level 2) threshold of 12 ppm [6]. When HF reacts with water, it generates heat and forms highly corrosive hydrofluoric acid. Upon absorption into the human body, HF binds with calcium and magnesium, forming insoluble salts. This process can lead to hypocalcemia and hypomagnesemia, which, in severe cases, may result in death [7,8].

AEGL (Acute Exposure Guideline Levels) and ERPG (Emergency Response Planning Guidelines) are critical standards used to evaluate the impact of acute chemical exposure on human health. AEGL, established by the U.S. Environmental Protection Agency (EPA), defines three levels (AEGL-1, AEGL-2, AEGL-3) based on severity, with AEGL-2 representing concentrations that may cause irreversible or serious health effects, potentially impairing escape ability [9]. ERPG, developed by the American Industrial Hygiene Association (AIHA), provides three exposure levels (ERPG-1, ERPG-2, ERPG-3), with ERPG-2 defining the concentration at which individuals might experience non-life-threatening but serious effects that do not impair self-rescue [10].

The impact of these toxic gases is particularly critical in confined spaces, as HF emissions tend to increase with the state of charge (SOC) of the battery [11]. Consequently, the recent trend of increasing battery capacity in electric vehicles necessitates additional safety measures. In South Korea, building codes mandate that electric vehicle parking facilities be located in underground parking garages, where fires during charging or parking often occur. Such incidents can trap smoke and toxic gases within enclosed spaces, exacerbating human casualties and complicating firefighting efforts.

This study focuses on the risk assessment of toxic gas dispersion caused by electric vehicle fires in underground apartment parking garages. Using the fire dynamics simulator (FDS), a computational fluid dynamics (CFD) software, the analysis models the emission and spread of toxic gases, including HF, from fires involving NCM lithium-ion batteries. Based on the 2020 report “Toxic Gases from Fire in Electric Vehicle” by RISE (Research Institutes of Sweden), the research evaluates the extent of the impact and risks associated with gas dispersion in confined spaces and examines the correlation between battery capacity and increased HF emissions.

## 2. Numerical Methods and Procedures

This study utilized FDS version 6.9.1 to evaluate the impact of toxic gas dispersion from electric vehicle fires in underground parking garages through computational fluid dynamics (CFD) analysis. The computational domain and the configuration of openings are shown in Figure 1 and Table 1. The simulation was conducted under natural ventilation conditions, where fresh air enters the domain through the main parking entrance (7.3 m × 3.0 m) and a permanently open window (4.0 m × 1.6 m) located adjacent to the entrance. The

three stairwell entrances also serve as passive ventilation pathways, allowing for the dispersion of toxic gases. No mechanical ventilation systems were considered in the model to evaluate the impact of purely natural ventilation. While the actual apartment building has 19 floors, modeling was limited to the stairwell up to the fourth floor due to computational constraints. The stairwell model may slightly differ from real-world conditions due to mesh limitations, but adjustments were made to maintain the same dimensions with minimal positional changes.

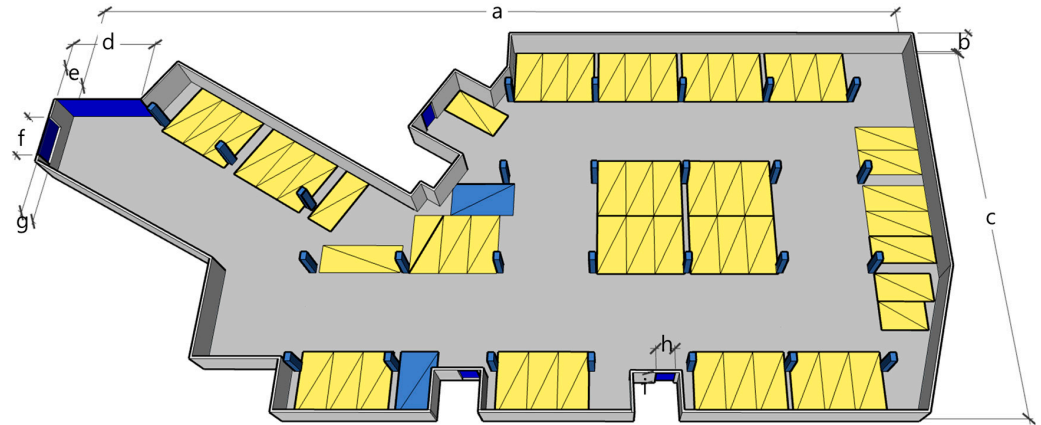


**Figure 1.** Schematics for the geometry of the three-dimensional simulation domain.

**Table 1.** Size of the computational domain and openings.

Domain					Opening			
a [m]	b [m]	c [m]	d [m]	e [m]	f [m]	g [m]	h [m]	i [m]
76.0	3.0	34.9	7.3	3.0	4.0	1.6	1.5	2.8

The initial conditions were set to standard ambient conditions, with an initial temperature of 293.15 K (20 °C) and an atmospheric pressure of 101.325 kPa throughout the computational domain. The initial concentration of toxic gases, including CO, HF, HCl, and HCN, was set to zero, assuming a clean air environment before ignition. The ignition source was modeled as a fixed heat release rate (HRR) applied at the fire location, following a predefined ramp function to simulate the fire growth phase.

In this study, the fire dynamics simulator (FDS) was employed to simulate fire dynamics and toxic gas dispersion in an underground parking garage. FDS numerically solves the low-Mach-number approximation of the Navier–Stokes equations for thermally driven, buoyancy-controlled flow. The governing equations used in our simulation include the following:

Mass conservation equation (continuity equation):

$$\frac{\partial \bar{\rho}}{\partial t} + \frac{\partial \bar{\rho} \tilde{u}_i}{\partial x_i} = 0 \quad (1)$$

Momentum conservation equation:

$$\frac{\partial \bar{\rho} \tilde{u}_i}{\partial t} + \frac{\partial}{\partial x_j} (\bar{\rho} \tilde{u}_i \tilde{u}_j) = -\frac{\partial \bar{p}}{\partial x_i} - \frac{\partial \bar{\tau}_{ij}}{\partial x_j} - \frac{\partial \tau_{ij}^{sgs}}{\partial x_j} + \bar{\rho} g_i \quad (2)$$

Energy conservation equation:

$$\frac{\partial \bar{\rho} \tilde{h}_s}{\partial t} + \frac{\partial (\bar{\rho} \tilde{u}_i \tilde{h}_s)}{\partial x_i} = \frac{D \bar{p}}{Dt} + \dot{q}''' - \frac{\partial q''_r}{\partial x_i} + \frac{\partial}{\partial x_i} \left( k \frac{\partial \tilde{T}}{\partial x_i} \right) + \sum_{\alpha} \frac{\partial}{\partial x_i} \left( \bar{\rho} D_{\alpha} \tilde{h}_{\alpha} \frac{\partial \tilde{Y}_{\alpha}}{\partial x_i} \right) \quad (3)$$

Species transport equation (toxic gas dispersion):

$$\frac{\partial(\bar{\rho}\tilde{Y}_\alpha)}{\partial t} + \frac{\partial(\bar{\rho}\tilde{u}_i\tilde{Y}_\alpha)}{\partial x_i} = -\frac{\partial}{\partial x_i}(\overline{\rho u_i Y_\alpha} - \bar{\rho}\tilde{u}_i\tilde{Y}_\alpha) + \frac{\partial}{\partial x_i}\left(\bar{\rho}D_\alpha\frac{\partial\tilde{Y}_\alpha}{\partial x_i}\right) + \bar{m}_\alpha''' \quad (4)$$

Equation of state:

$$\rho = \frac{\bar{p}\bar{W}}{RT} \quad (5)$$

This equation relates pressure, density, and temperature, assuming the ideal gas law.

In our simulation, we utilized large eddy simulation (LES) for turbulence modeling, which effectively captures the unsteady nature of fire-induced flow. The eddy dissipation concept (EDC) model was employed for combustion chemistry, ensuring accurate predictions of flame propagation and toxic gas generation. Radiation heat transfer was handled using the gray gas model, which solves the radiative transport equation to account for thermal radiation effects in the fire environment. The detailed descriptions of the governing equation are in Ref. [12].

The computational domain was discretized using a structured mesh with a uniform grid size of 0.2 m to balance computational efficiency and accuracy. Given the complex fire dynamics in confined spaces, a grid independence study was conducted by comparing the results for three different grid resolutions (0.3 m, 0.2 m, and 0.1 m). The analysis confirmed that further refinement beyond 0.2 m did not lead to significant variations in temperature and gas concentration distributions, indicating that the chosen resolution was sufficient for capturing fire-induced flow characteristics. This resolution also aligns with the recommended  $D/dx \leq 10$  criteria for FDS simulations, ensuring adequate resolution for fire dynamics modeling.

The modeling was based on the worst-case scenario of Electric Vehicle B, as identified in the RISE report, which included three scenarios: Internal Combustion Engine Vehicle A, Electric Vehicle A, and Electric Vehicle B. The worst-case scenario was selected due to its highest total heat release (THR) of 6.7 GJ and the largest HF emission of 859 g.

It is challenging to apply a chemical reaction mechanism that quantitatively matches the release of all toxic species observed in actual electric vehicle fires, considering the wide range of chemicals addressed in this study. Therefore, in this research, the heat release rate obtained from previous experiments [4], along with the corresponding chemical species concentrations, was directly used as an input condition for the FDS calculations as shown in Table 2. Specifically, the experimental conditions for the given heat release rate were used as shown in Figure 2 to define the heat generation rate as a time-dependent function of fuel mass flux, and the considered chemical species were released from the location of the EV's lower battery in proportion to the heat release rate, ensuring that the final emission quantities matched the values obtained from the experiments.

**Table 2.** Gas compounds measured from the exhaust duct.

Type of Vehicle		BEV B
Total heat release [GJ]		6.7
	CO <sub>2</sub> [kg]	438
Amount of toxic gas released	CO [g]	9510
	HF [g]	859
	HCl [g]	1800
	HCN [g]	155
	SO <sub>2</sub> [g]	645
	NO [g]	617
	NO <sub>2</sub> [g]	76



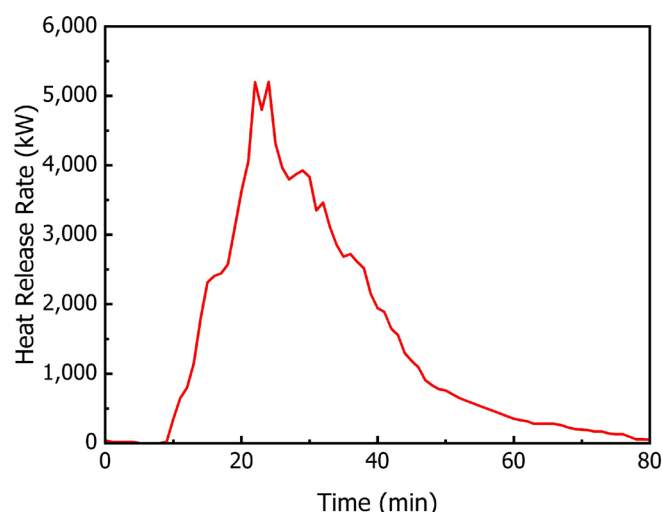


**Figure 2.** Heat release rate curve as a function of time for BEV B.

In the simulations of this study, polyurethane was used as the fuel for the electric vehicle fire. However, since the focus was on matching the heat release rate, the choice of polyurethane as the fuel component did not hold any particular significance. For clarity, preliminary simulations conducted prior to this study confirmed that the heat release rate and the corresponding chemical species concentrations were accurately reproduced.

The fire model used polyurethane as the fuel, following performance-based design standards. The heat release rate per unit area (HRRPUA) was set based on the heat release rate graph measured during real vehicle fire experiments, using a flame area of 3 m<sup>2</sup> located beneath the vehicle. The ramp function was employed to align the total heat release with real fire conditions. Toxic gases generated during the fire (HF, HCl, HCN, CO, NO, NO<sub>2</sub>, SO<sub>2</sub>) were simulated by releasing a mixture of seven gases through a vent beneath the vehicle. The total emission of each toxic substance was calibrated to match real fire experiment measurements (over 99.8% consistency) using mass flux and ramp adjustments. Carbon dioxide emissions were directly modeled based on the combustion of polyurethane.

Two primary fire scenarios were considered:

1. Fire ignition near Stairwell 3 (Ignition Point 1).
2. Fire ignition near the main entrance of the underground parking garage (Ignition Point 2).

Concentration sensors were placed at heights of 1.5 m and 1.8 m above the parking garage floor, reflecting the locations of human respiratory pathways and head height, to measure toxic gas concentrations. For the stairwell, modeling was performed up to the fourth floor, and beyond that, vents were added to facilitate the escape of smoke and toxic gases generated during the electric vehicle fire. Concentration measurements were conducted at 1.5 m and 1.8 m above the landings of each stairwell floor to assess the risks posed by toxic gases. The locations of the electric vehicle, concentration sensors, and slices for each fire scenario are illustrated in Figure 3.

Simulations were conducted for the following scenarios:

- A 24 kWh electric vehicle fire near the main entrance (Ignition Point 2), expected to have the smallest impact on toxic gas dispersion.
- A 24 kWh electric vehicle fire near Stairwell 3 (Ignition Point 1), expected to result in greater toxic gas dispersion and impact.

Additionally, scenarios reflecting the recent trend of increasing battery capacities in electric vehicles were modeled using 53 kWh and 99.8 kWh lithium-ion batteries. These

scenarios incorporated corresponding increases in hydrogen fluoride emissions. Details of battery capacities and HF emissions for each scenario are provided in Table 3.

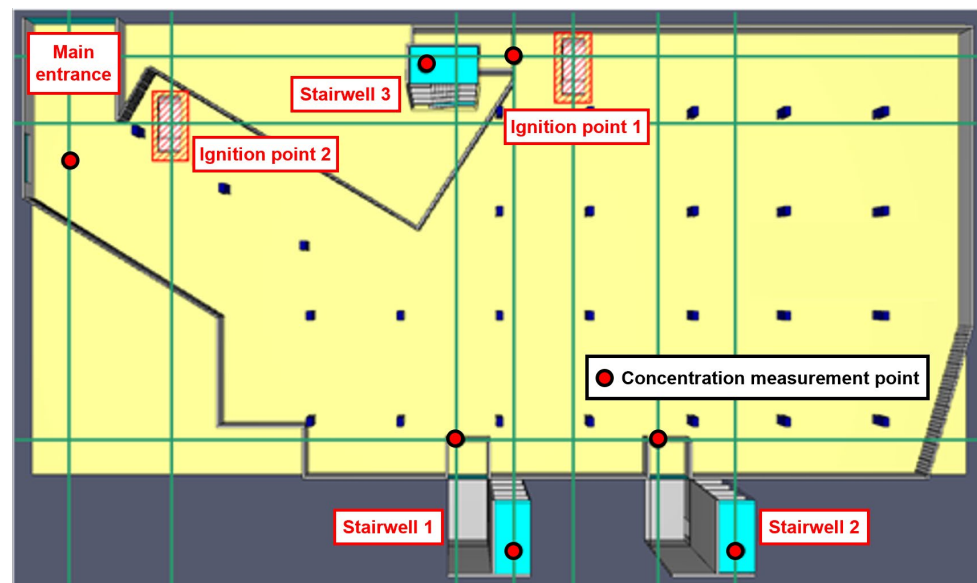


**Figure 3.** Ignition points (entrance, near Stairwell 3) and gas measuring sensor points.

**Table 3.** Battery capacity and amount of hydrogen fluoride emissions by fire scenario.

Case	Ignition Point	Battery Capacity [kWh]	HF [g]	Total Heat Release [GJ]
1	Entrance	24	859	6.7
2	Stairwell 3	24	859	6.7
3	Stairwell 3	53	1729	8.1
4	Stairwell 3	99.8	3133	10.4

The relationship between increased HF emissions and total heat release due to larger battery capacities was derived using empirical correlations from the RISE report's combustion experiments on individual lithium-ion batteries. These relationships are illustrated in Figures 4 and 5 [13].

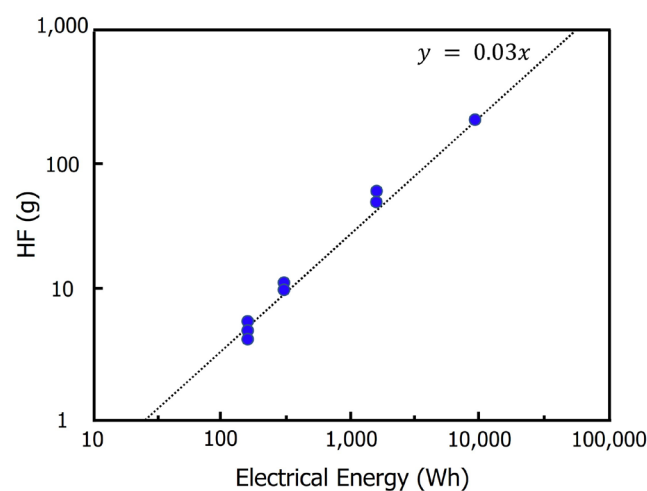


**Figure 4.** Correlation between hydrogen fluoride emission and battery capacity [6].

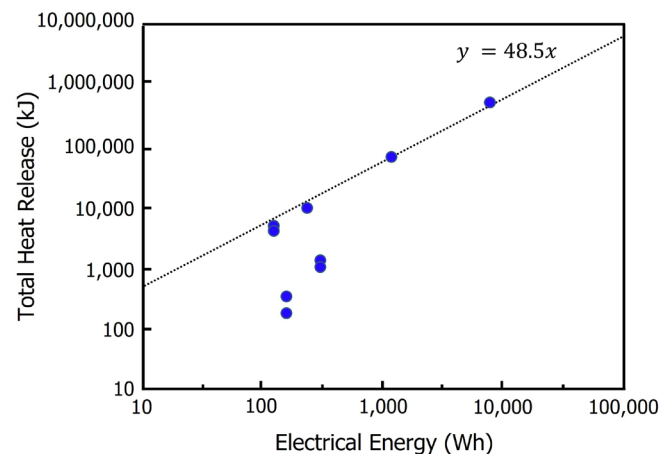


**Figure 5.** Correlation between total heat release and battery capacity [6].

### 3. Results and Discussion

Based on the RISE report, we conducted a risk assessment of toxic gas dispersion during electric vehicle (EV) fires using the fire dynamics simulator (FDS). The assessment focused on gas concentrations resulting from toxic gas emissions. The ability of individuals to maintain cognitive functions and evacuate safely when exposed to fire is defined as tenability. The time to compromised tenability refers to the shortest duration among four factors: exposure to asphyxiant gases (substances that impede oxygen delivery to the lungs or circulation), irritant gases (highly acidic substances causing irritation and acid burns), heat, and reduced visibility due to smoke.

#### 3.1. Hydrogen Fluoride Concentrations and Distributions

Figure 6 illustrates the HF concentration distribution when a 24 kWh battery EV fire occurs near the main entrance (Ignition Point 2). Figure 6a,b depict the horizontal and vertical HF concentration distributions in the underground parking lot approximately 26 min post-ignition. Figure 7a,b shows the temporal variation of HF concentrations at each stairwell entrance and within Stairwell 1 across different floors.

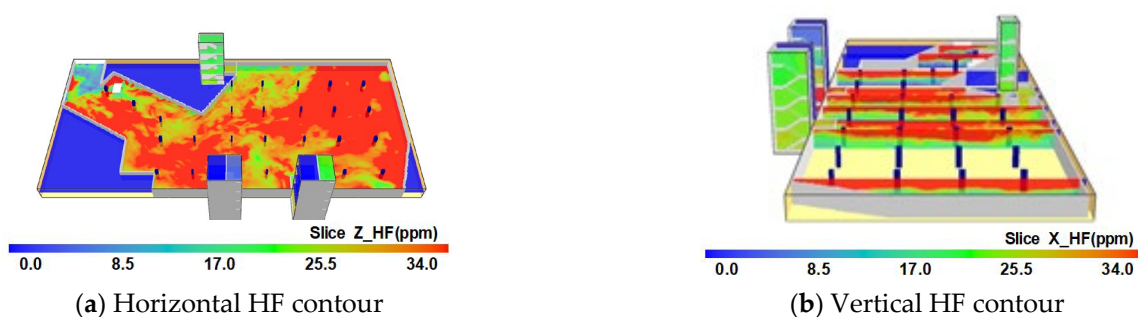


**Figure 6.** HF concentrations for (a) horizontal areas and (b) vertical regions in an underground parking garage during a 24 kWh EV fire at Ignition Point 2.

The simulation results indicate that natural ventilation plays a critical role in mitigating toxic gas accumulation. In scenarios where ventilation openings were limited, HF concentrations in confined areas exceeded 488.2 ppm, surpassing AEGL-2 thresholds for human exposure. Comparatively, well-ventilated zones exhibited significantly lower toxic gas concentrations, suggesting that strategic placement of ventilation pathways can effectively reduce hazardous gas buildup.

The HF concentration at the main entrance and stairwell entrances peaked around 1450 s across all measurement points. Near the main entrance fire, the highest HF concentration

was recorded at the Stairwell 1 entrance (maximum 45.0 ppm). However, the concentration exceeded the AEGL-2 (30 min) threshold of 34 ppm for only about 439 s (7 min and 19 s), remaining below the exposure limit. This suggests that the smaller battery capacity resulted in lower HF emissions during the fire. Within Stairwell 1, HF concentrations temporarily exceeded the AEGL-2 (30 min) threshold but did not sustain for 30 min.

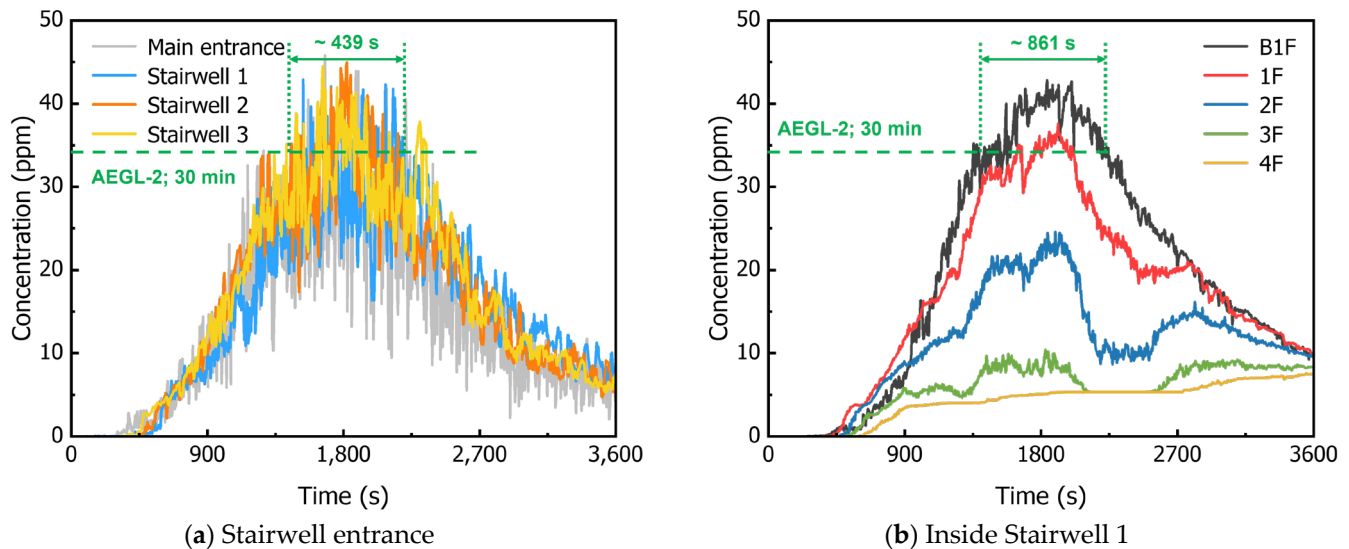


**Figure 7.** HF concentrations as a function of time at (a) each stairwell entrance and (b) inside Stairwell 1 for a 24 kWh EV fire at Ignition Point 2.

Figures 8 and 9 present the horizontal (at a height of 1.8 m) and vertical HF concentration distributions and their temporal variations at each entrance and within Stairwell 3 when a 24 kWh EV fire occurs near Stairwell 3 (Ignition Point 1). In this scenario, the highest HF concentration was observed at the Stairwell 3 entrance (maximum 148.2 ppm), exceeding the AEGL-2 (30 min) threshold for approximately 1952 s (32 min and 32 s). With the stairwell doors assumed open, HF concentrations within Stairwell 3 also surpassed the AEGL-2 (30 min) threshold but did not maintain for 30 min, sustaining for about 1462 s (24 min and 22 s). This indicates that HF concentration decreases with distance from the ignition point due to slower vertical dispersion compared to smoke movement.

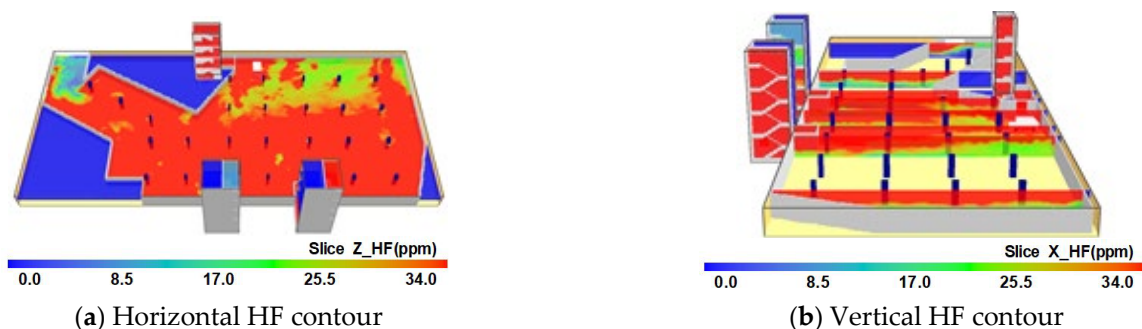


**Figure 8.** HF concentrations for (a) horizontal areas and (b) vertical regions in an underground parking garage during a 24 kWh EV fire at Ignition Point 1.

We compared scenarios where EV fires with larger battery capacities occurred at Ignition Point 1. Figures 10 and 11 illustrate the temporal HF concentration variations for 53 kWh and 99.8 kWh battery EV fires, respectively. Figures 10a and 11a show HF concentration changes over time at each stairwell entrance, while Figures 10b and 11b depict HF concentrations within Stairwell 3 across different floors.

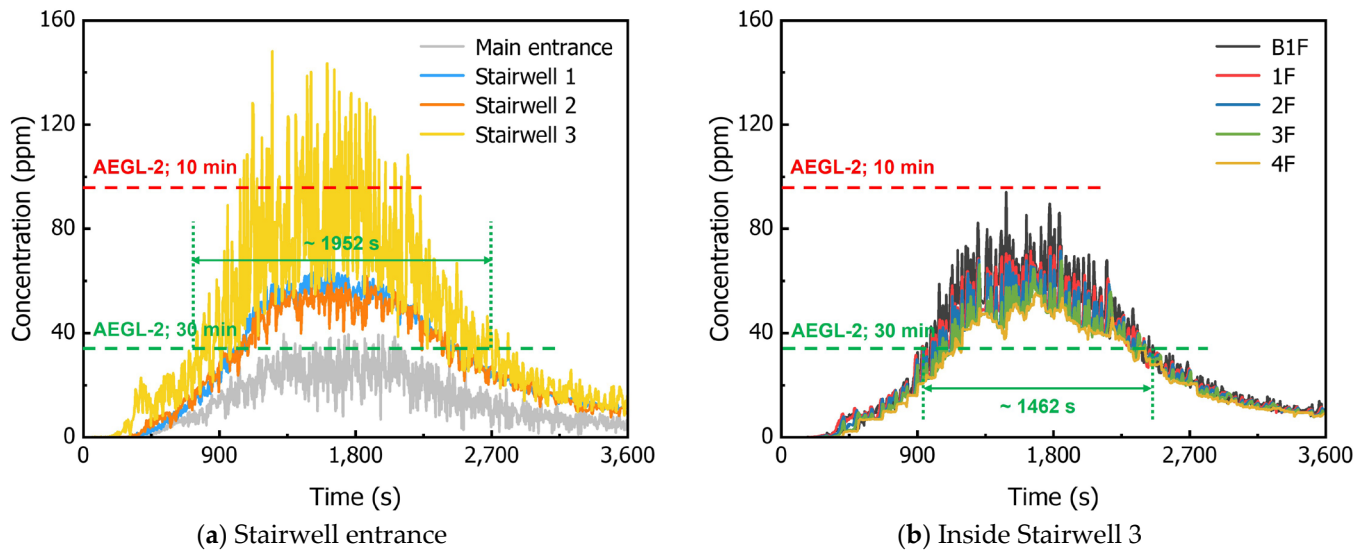


**Figure 9.** HF concentrations as a function of time at (a) each stairwell entrance and (b) inside Stairwell 3 for a 24 kWh EV fire at Ignition Point 1.

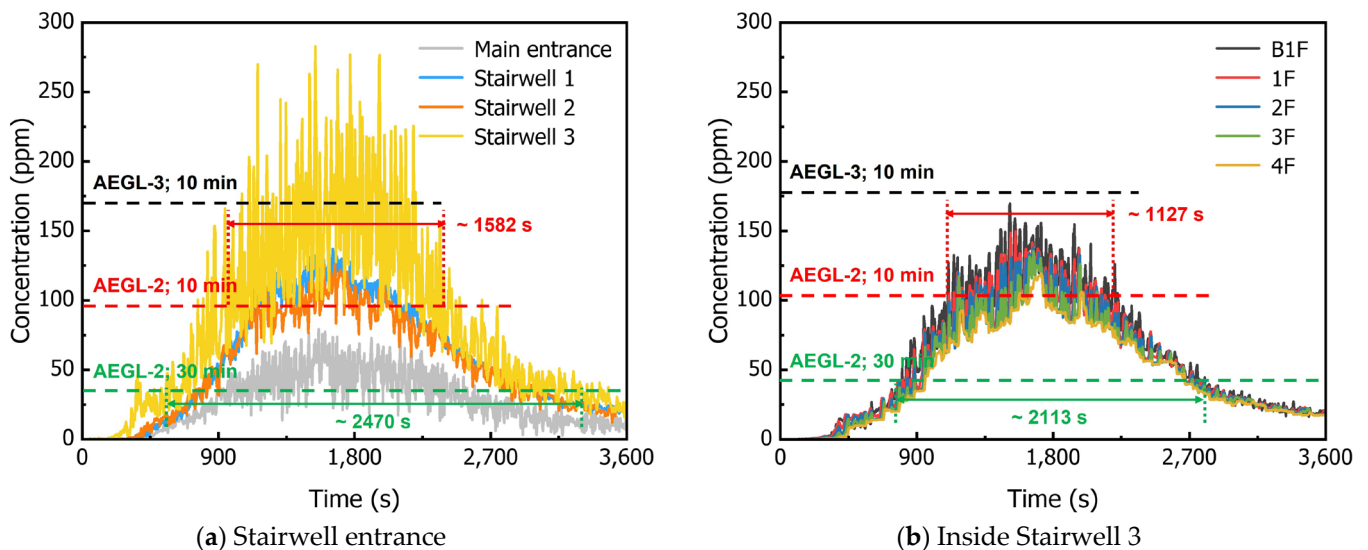


**Figure 10.** HF concentrations as a function of time at (a) each stairwell entrance and (b) inside Stairwell 3 for a 53 kWh EV fire at Ignition Point 1.

For the 53 kWh battery EV fire near Stairwell 3, the highest HF concentration was at Stairwell 3 entrance (maximum 282.9 ppm), exceeding the AEGL-2 (30 min) threshold for about 2470 s (41 min and 10 s), and the AEGL-2 (10 min) threshold of 95 ppm for approximately 1580 s (26 min and 20 s). Within Stairwell 3, HF concentrations exceeded the AEGL-2 (30 min) threshold for about 2113 s (35 min and 13 s) and the AEGL-2 (10 min) threshold for approximately 1127 s (18 min and 47 s).

In the case of the 99.8 kWh battery EV fire near Stairwell 3, the highest HF concentration at Stairwell 3 entrance was 488.2 ppm, exceeding the AEGL-2 (30 min) threshold for about 3229 s (53 min and 49 s) and the AEGL-2 (10 min) threshold for approximately 2099 s (34 min and 59 s). Notably, the AEGL-3 (10 min) threshold of 170 ppm was also exceeded for over 17 min, indicating significant variability in measurements and necessitating further research. Within Stairwell 3, HF concentrations surpassed the AEGL-2 (30 min) threshold for about 2840 s (47 min and 20 s), the AEGL-2 (10 min) threshold for approximately 1735 s (28 min and 55 s), and the AEGL-3 (10 min) threshold for about 875 s (14 min and 35 s).



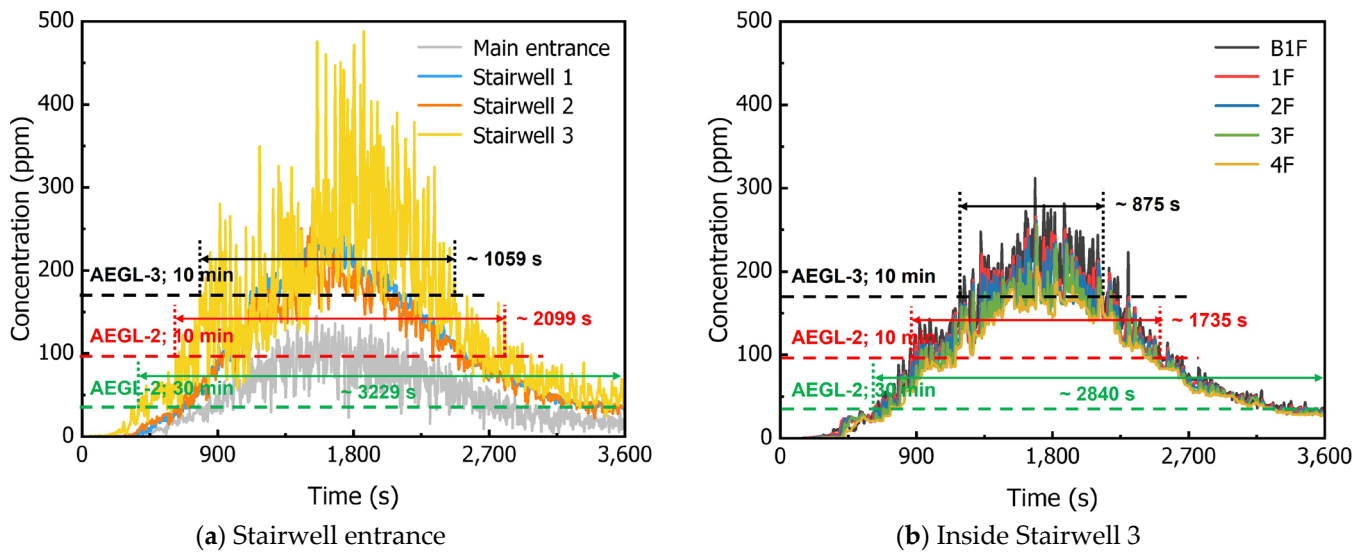


**Figure 11.** HF concentrations as a function of time at (a) each stairwell entrance and (b) inside Stairwell 3 for a 99.8 kWh EV fire at Ignition Point 1.

The variation in HF concentrations across different zones is influenced by multiple factors, primarily fire location, ventilation conditions, and the structural characteristics of the underground parking garage. Fires near well-ventilated areas, such as Ignition Point 2 (near the main entrance), exhibited lower HF concentrations due to natural airflow diluting the toxic gases more effectively. In contrast, Ignition Point 1, located in a poorly ventilated zone, led to higher HF accumulation as the restricted airflow hindered gas dispersion. Additionally, the geometric structure of the underground parking garage played a significant role in gas movement. Certain areas with limited airflow acted as gas accumulation zones, resulting in localized peaks in HF concentration. These findings underscore the importance of ventilation and spatial configuration in managing toxic gas dispersion during electric vehicle fires in confined spaces.

### 3.2. Analysis of Fractional Effective Dose and Concentration

In this study, we analyzed the fractional effective dose (FED) for asphyxiant gases (CO, HCN) and the fractional effective concentration (FEC) for irritant gases (HCl, HF, NO, SO<sub>2</sub>) during fire incidents across various battery capacities [10]. The fractional effective dose (FED) for asphyxiant gases such as carbon monoxide (CO) and hydrogen cyanide (HCN) is calculated as a cumulative measure over a specified time interval,  $t_1$  to  $t_2$ , using the following Equation (6) [14,15]:

$$X_{FED} = \sum_{t_1}^{t_2} \frac{\varphi_{CO} \times v_{CO_2}}{35000} \Delta t + \sum_{t_1}^{t_2} \frac{(\varphi_{HCN} \times v_{CO_2})^{2.36}}{1.2 \times 10^6} \Delta t \quad (6)$$

where  $\varphi_{CO}$  is the average concentration of carbon monoxide (in ppm) during the time increment  $\Delta t$ .  $\varphi_{HCN}$  is the average concentration of HCN (in ppm) during  $\Delta t$ .  $\Delta t$  is the time increment. In each time increment, the  $\varphi_{CO}$  and  $\varphi_{HCN}$  terms in Equation (6) are multiplied by a frequency factor  $v_{CO_2}$  to account for the accelerated inhalation of asphyxiant gases due to hyperventilation. This consideration is crucial, as exposure to asphyxiant gases like CO and HCN can lead to hypoxia, resulting in central nervous system depression, unconsciousness, and potentially fatal outcomes.

$$v_{CO_2} = \exp\left(\frac{\varphi_{CO_2}}{5}\right) \quad (7)$$



where  $\varphi_{\text{CO}_2}$  is the average volumetric percentage of carbon dioxide over time. An  $X_{\text{FED}}$  value of 1 indicates that 50% of the general population would experience compromised tenability at that exposure level. For design purposes, a threshold of 0.3 is recommended, signifying that 11% of the general population (including individuals with underlying health conditions) would lose tenability. In more conservative approaches, a threshold of 0.1 may be applied, representing 1% of the general population experiencing compromised tenability [4,13].

The analysis of fractional effective dose (FED) for asphyxiant gases, specifically CO and HCN, is crucial because exposure to these gases typically leads to hypoxia—a reduction in oxygen supply or utilization within body tissues. This condition can result in central nervous system depression, unconsciousness, and, ultimately, death.

In this study, the fractional effective concentration (FEC) for irritant gases (HCl, HF, NO, SO<sub>2</sub>) was calculated at each discrete time increment, rather than as a cumulative measure like the FED. Since the model includes these specific irritant gases, the FEC was determined using Equation (8) [14,15].

$$X_{\text{FEC}} = \frac{\varphi_{\text{HCl}}}{F_{\text{HCl}}} + \frac{\varphi_{\text{HF}}}{F_{\text{HF}}} + \frac{\varphi_{\text{NO}}}{F_{\text{NO}}} + \frac{\varphi_{\text{SO}_2}}{F_{\text{SO}_2}} \quad (8)$$

where  $\varphi$  is the average concentration of irritant gases (in ppm).  $F$  is the concentration of irritant gases (in ppm) expected to significantly compromise occupant survivability ( $F_{\text{HCl}}$ : 1000 ppm,  $F_{\text{HF}}$ : 500 ppm,  $F_{\text{NO}}$ : 250 ppm, and  $F_{\text{SO}_2}$ : 150 ppm).

Similar to the  $X_{\text{FED}}$ , a  $X_{\text{FEC}}$  value of 1 indicates that 50% of the general population would experience compromised tenability at that exposure level. For design purposes, a threshold of 0.3 is recommended, signifying that 11% of the general population (particularly those with underlying health conditions) would lose tenability. A more conservative approach may adopt a threshold of 0.1, indicating that 1% of the general population would experience compromised tenability.

According to the literature [13], in contrast to the direct effects of asphyxiant gases (CO, HCN), the impact of exposure to irritant gases (HCl, HF, NO, SO<sub>2</sub>) is more complex. Generally, exposure can lead to irritation of the eyes, upper respiratory tract (nose, throat, larynx), and lungs, causing symptoms such as tearing, blinking, discomfort in the eyes, nose, and mouth, chest tightness, coughing, respiratory arrest, laryngeal spasm, bronchoconstriction, and dyspnea, depending on individual sensitivity. Understanding this, the XFED and XFEC values defined earlier can be effectively used to evaluate the impact of toxic gases on humans.

The FED and FEC were measured at a height of 1.8 m above the floor of the underground parking garage, representing head height. As previously mentioned, FED is a cumulative measure, while FEC reflects concentration levels, accounting for instantaneous effects at a given time. Figures 12–14 present graphs of FED and FEC values analyzed for each battery capacity.

For the fractional effective dose values, a design threshold of 0.3 is recommended. Analysis indicates that as battery capacity increases, the time to reach an FED value exceeding 0.3 decreases across all stairwells (Stairwells 1, 2, and 3). Specifically, larger battery capacities and closer proximity to the ignition source result in shorter times to reach this threshold. The tenability time concerning asphyxiant gases (CO, HCN) ranges from a minimum of 15 min and 22 s (in Stairwell 3 during a 99.8 kWh battery fire) to a maximum of 20 min and 35 s (in Stairwell 1 during a 24 kWh battery fire). Therefore, occupants must evacuate the affected area within this timeframe to avoid exposure to hazardous gases.

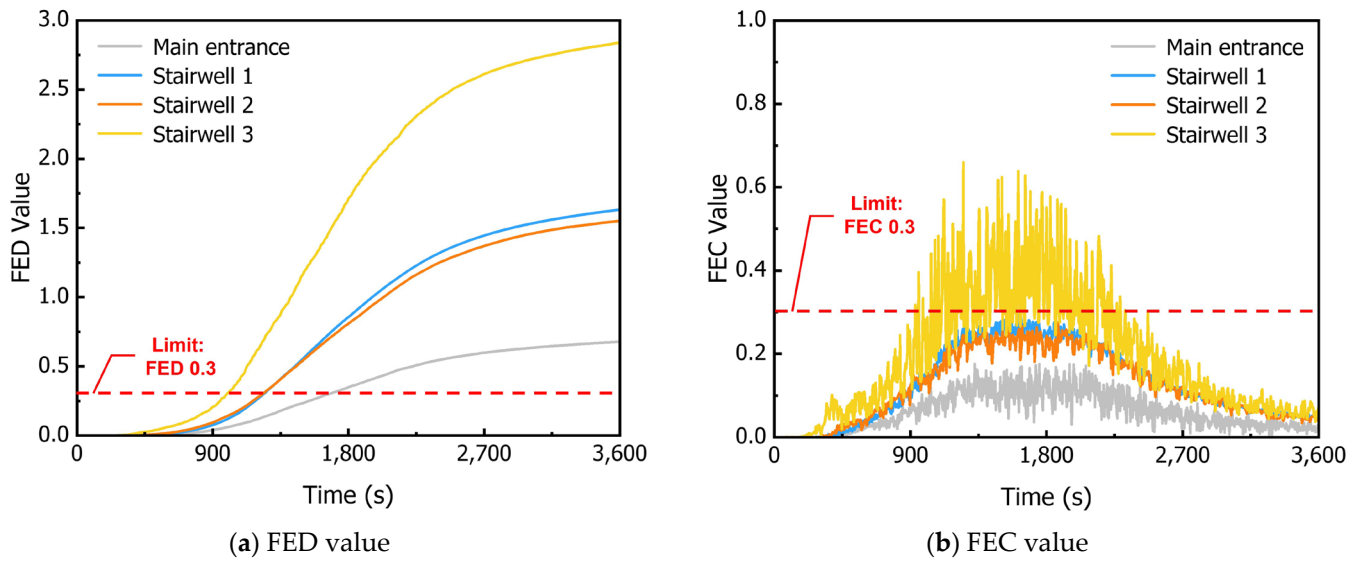


**Figure 12.** Fractional effective dose (FED) and fractional effective concentration (FEC) for a 24 kWh EV fire at Ignition Point 1.

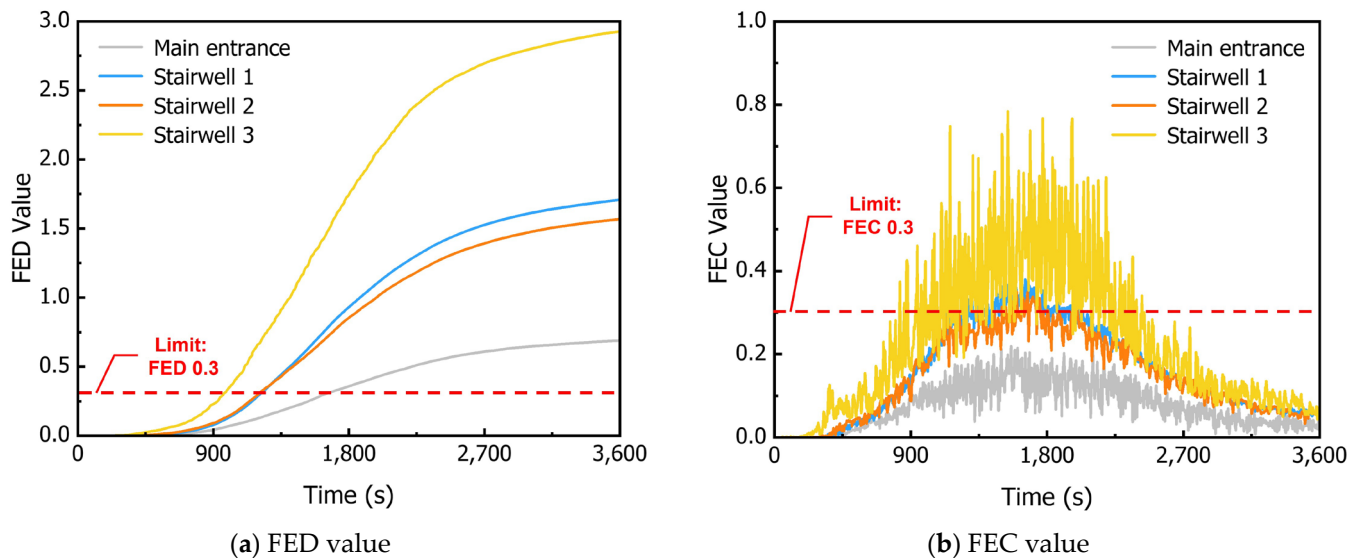


**Figure 13.** Fractional effective dose (FED) and fractional effective concentration (FEC) for a 53 kWh EV fire at Ignition Point 1.

The fractional effective concentration value is also recommended to use a threshold of 0.3 for general design levels. Based on this criterion, it was observed that in all three stairwells (1, 2, and 3), as the battery capacity increased, the time to reach an FEC value exceeding 0.3 decreased. This indicates that larger battery capacities and closer proximity to the ignition source result in shorter times to reach the threshold value. However, in the case of the smallest fire scenario with a 24 kWh battery, it was noted that Stairwells 1 and 2 did not reach this threshold value.

The difference in trends between FED and FEC across different battery capacities can be attributed to the distinct characteristics of asphyxiant and irritant gases. Asphyxiant gases (CO, HCN) are released in relatively proportional amounts regardless of battery capacity, leading to minimal variation in FED values. In contrast, irritant gases (HF, HCl) exhibit a stronger correlation with battery capacity, as their production is linked to the decomposition of battery electrolytes. As the battery capacity increases, the total heat release (THR) rises, accelerating electrolyte breakdown and significantly increasing HF

and HCl emissions. This explains why FEC values show a more pronounced difference between Figures 12 and 13, while FED remains relatively stable.

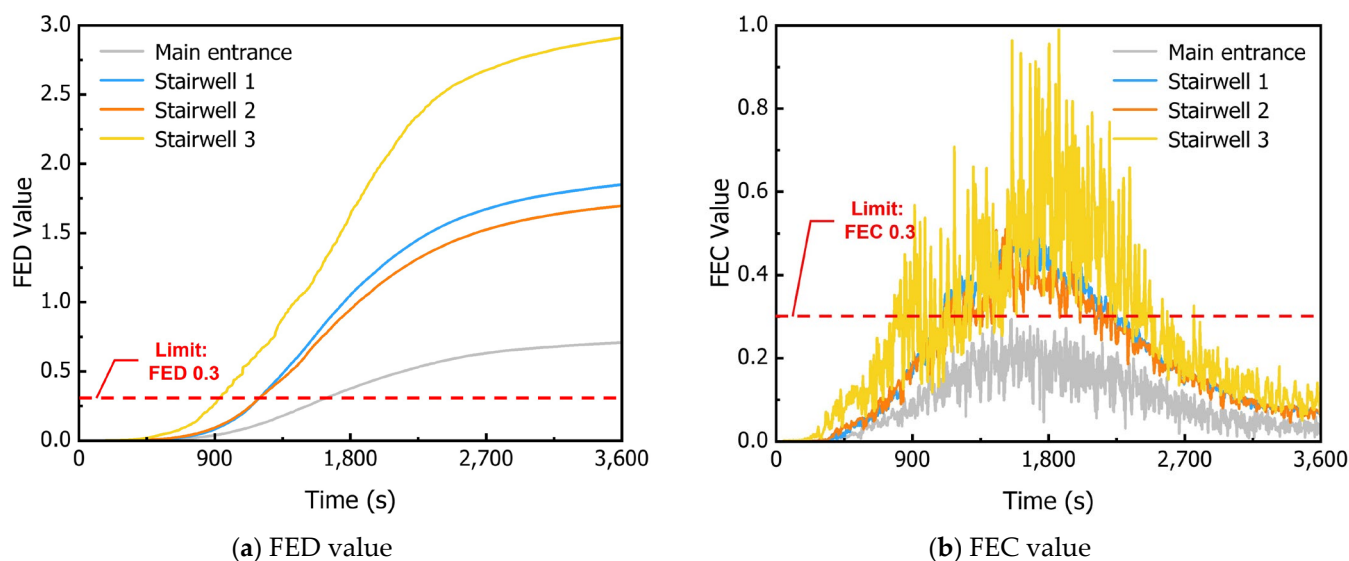


**Figure 14.** Fractional effective dose (FED) and fractional effective concentration (FEC) for a 99.8 kWh EV fire at Ignition Point 1.

Regarding the time to compromised tenability due to irritant toxic gases (HCl, HF, NO, SO<sub>2</sub>), it was found that occupants needed to evacuate the affected area within a minimum of 13 min and 23 s (Stairwell 3, 99.8 kWh fire) to a maximum of 26 min and 46 s (Stairwell 2, 53 kWh fire) after the fire outbreak.

Figure 15 shows the exposure limit time for FED and FEC values for three battery capacities and stairwell locations. As shown in Figure 15, increasing battery capacity results in a shorter time to reach the FED and FEC threshold of 0.3. Additionally, Stairwell 3, being closest to the electric vehicle ignition source, consistently exhibits the shortest time to reach these thresholds. This indicates a proportional relationship whereby larger battery capacities and closer proximity to the ignition source lead to greater harm from toxic gases.

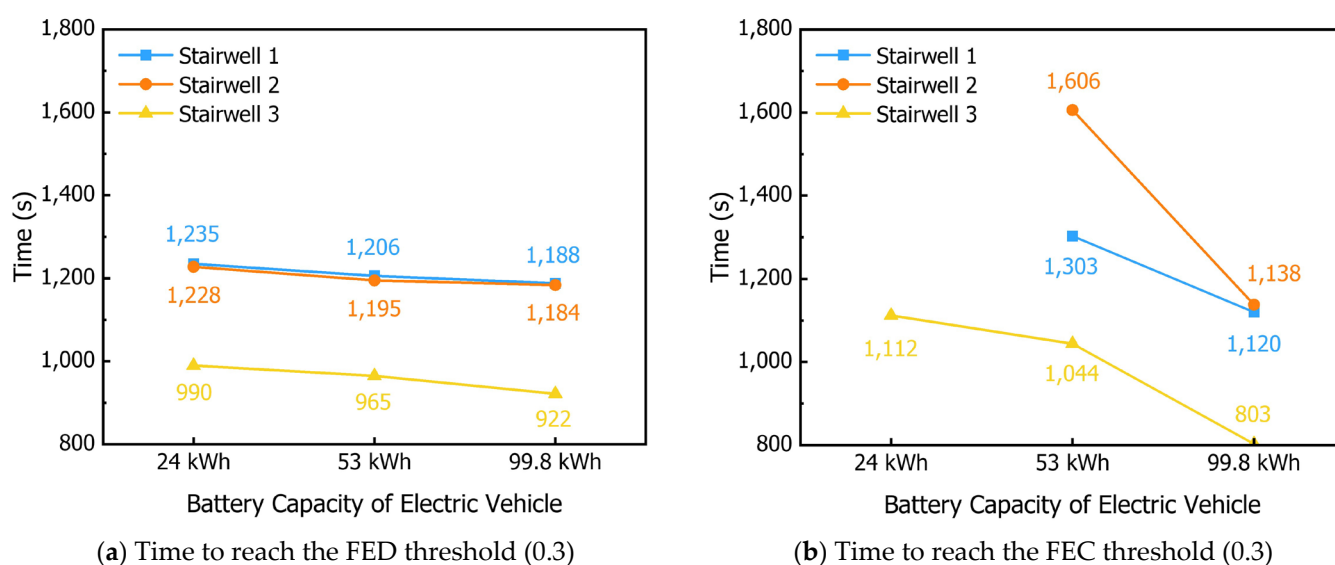


**Figure 15.** Exposure time limit for (a) FED and (b) FEC for three battery capacities and stairwell locations.

## 4. Conclusions

This study conducted a comprehensive risk assessment of toxic gas dispersion, particularly hydrogen fluoride (HF), caused by electric vehicle fires in underground apartment parking garages. Through numerical analysis using the fire dynamics simulator (FDS), the findings revealed that the extent of toxic gas dispersion is significantly influenced by factors such as battery capacity, fire location, and ventilation conditions. Larger battery capacities, modeled up to 99.8 kWh, resulted in HF concentrations exceeding acute exposure guideline thresholds, reducing the time to compromised tenability and escalating risks for occupants and emergency responders.

The results underscore the critical need for improved fire safety strategies tailored to confined environments. Measures such as optimizing ventilation systems, developing battery-specific fire suppression technologies, and reinforcing building codes for underground parking structures are essential to mitigate the risks associated with electric vehicle fires. Furthermore, the study highlights the importance of rapid evacuation plans and emergency response protocols to protect human lives in such scenarios.

By addressing the challenges posed by the increasing prevalence of high-capacity electric vehicles, this research contributes valuable insights toward advancing fire safety guidelines and ensuring the safe integration of electric vehicles into urban infrastructure.

To enhance fire safety and extend evacuation time in underground parking garages, early fire detection systems, such as smoke detectors and gas sensors inside vehicles and buildings, should be considered as a potential mitigation strategy. The effectiveness of such systems, however, depends on regulatory standards that may vary across regions.

**Author Contributions:** J.J. (Jiseong Jang): methodology, validation, formal analysis, investigation, writing—original draft preparation; J.J. (Joonho Jeon): writing—original draft preparation, writing—review and editing, funding acquisition; C.B.O.: conceptualization, supervision, writing—review and editing, funding acquisition. All authors have read and agreed to the published version of the manuscript.

**Funding:** This research was supported by the “Regional Innovation Strategy (RIS)” through the National Research Foundation of Korea (NRF), funded by the Ministry of Education (MOE) (2023RIS-007).

**Institutional Review Board Statement:** Not applicable.

**Informed Consent Statement:** Not applicable.

**Data Availability Statement:** Not applicable.

**Acknowledgments:** This paper is a revised and supplemented version of the master’s thesis by Jiseong Jang from the Graduate School of Industry at Pukyong National University.

**Conflicts of Interest:** The authors declare no conflicts of interest.

## Abbreviations

The following abbreviations are used in this manuscript:

AEGL-2	Acute Exposure Guideline Level 2
CFD	computational fluid dynamics
ERPG-2	Emergency Response Planning Guideline Level 2
EV	electric vehicle
FDS	fire dynamics simulator
FEC	fractional effective concentration
FED	fractional effective dose
HF	hydrogen fluoride
HRRPUA	heat release rate per unit area
SOC	state of charge
THR	total heat release

## References

1. Ministry of Land, Infrastructure and Transport (MOLIT). Vehicle Registration Statistics by Year. Korea Transportation Statistics. 2023. Available online: <https://stat.molit.go.kr> (accessed on 31 December 2024).
2. National Fire Agency Research Center (NFARC). *Electric Vehicle Fire Response Guide*; Korea National Fire Agency: Sejong-si, Republic of Korea, 2023.
3. Li, W.; Rao, S.; Xiao, Y.; Gao, Z.; Chen, U.; Wang, H.; Ouyang, M. Fire boundaries of lithium-ion cell eruption gases caused by thermal runaway. *iScience* **2021**, *24*, 102401. [[CrossRef](#)] [[PubMed](#)]
4. Larsson, F.; Andersson, P.; Blomqvist, P.; Mellander, B.E. Toxic fluoride gas emissions from lithium-ion battery fires. *Sci. Rep.* **2017**, *7*, 10018. [[CrossRef](#)] [[PubMed](#)]
5. Hynynen, J.; Willstrand, O.; Blomqvist, P.; Andersson, P. Analysis of combustion gases from large-scale electric vehicle fire tests. *Fire Saf. J.* **2023**, *139*, 103829. [[CrossRef](#)]
6. Yoon, C.S. Emergency standards for chemical substances (leakage and accidents). *J. Korean Soc. Occup. Environ. Hyg.* **2016**, *26*, 22–31.
7. Korea Occupational Safety and Health Agency (KOSHA). *KOSHA Guide H-123-2013: Guidelines for Prevention of Intoxication and Emergency Response for Workers Handling Hydrofluoric Acid and Hydrogen Fluoride*; Korea Occupational Safety and Health Agency: Ulsan, Republic of Korea, 2013.
8. Subcommittee on Acute Exposure Guideline Levels, Committee on Toxicology, Board on Environmental Studies and Toxicology. *Acute Exposure Guideline Levels for Selected Airborne Chemicals (Vol. 4)*; National Academies Press: Washington, DC, USA, 2004.
9. U.S. Environmental Protection Agency (EPA). Acute Exposure Guideline Levels (AEGLs). 2022. Available online: <https://www.epa.gov/aegl> (accessed on 1 December 2024).
10. American Industrial Hygiene Association (AIHA). Emergency Response Planning Guidelines (ERPGs). 2016. Available online: <https://www.aiha.org/get-involved/erpg> (accessed on 1 December 2024).
11. Larsson, F.; Andersson, P.; Blomqvist, P.; Lorén, A.; Mellander, B.E. Characteristics of lithium-ion batteries during fire tests. *J. Power Sources* **2014**, *271*, 414–420. [[CrossRef](#)]
12. Myilsamy, D.; Oh, C.B.; Choi, B.I. Large Eddy Simulation of the Backdraft Dynamics in Compartments with Different Opening Geometries. *J. Mech. Sci. Technol.* **2019**, *33*, 2111–2121. [[CrossRef](#)]
13. Willstrand, O.; Bisschop, R.; Blomqvist, P.; Temple, A.; Anderson, J. *Toxic Gases from Fire in Electric Vehicles*; RISE Report 2020:90; RISE Research Institutes of Sweden: Borås, Sweden, 2020.
14. *ISO 13571:2012; Life-Threatening Components of Fire—Guidelines for the Estimation of Time to Compromised Tenability in Fires*. International Organization for Standardization: Geneva, Switzerland, 2012.
15. Yang, P.; Yang, L.; Ju, X.; Liao, B.; Ye, K.; Li, L.; Cao, B.; Ni, Y. A comprehensive investigation on the thermal and toxic hazards of large format lithium-ion batteries with LiFePO<sub>4</sub> cathode. *J. Hazard. Mater.* **2020**, *381*, 120916. [[CrossRef](#)]

**Disclaimer/Publisher’s Note:** The statements, opinions and data contained in all publications are solely those of the individual author(s) and contributor(s) and not of MDPI and/or the editor(s). MDPI and/or the editor(s) disclaim responsibility for any injury to people or property resulting from any ideas, methods, instructions or products referred to in the content.